Global Ecology and Biogeography, (Global Ecol. Biogeogr.) (2016) 25, 1489–1499

A Journal of Macroecology

Global Ecology and Biogeography

RESEARCH PAPER

Ant assemblages have darker and larger members in cold environments

Tom R. Bishop[1,2*], Mark P. Robertson[2], Heloise Gibb[3], Berndt J. van Rensburg[4,5], Brigitte Braschler[6,7], Steven L. Chown[8], Stefan H. Foord[9], Thinandavha C. Munyai[9,10], Iona Okey[3], Pfarelo G. Tshivhandekano[2], Victoria Werenkraut[11] and Catherine L. Parr[1,12]

[1]Department of Earth Ocean and Ecological Sciences, University of Liverpool, Liverpool, L69 3GP, UK, [2]Centre for Invasion Biology, Department of Zoology and Entomology, University of Pretoria, Pretoria, 0002, South Africa, [3]Department of Zoology, La Trobe University, Melbourne, Vic. 3068, Australia, [4]School of Biological Sciences, University of Queensland, St Lucia, Qld 4072, Australia, [5]Department of Zoology, Centre for Invasion Biology, University of Johannesburg, Auckland Park, Johannesburg, 2006, South Africa, [6]Department of Botany and Zoology, Centre for Invasion Biology, Stellenbosch University, Matieland, South Africa, [7]Section of Conservation Biology, Department of Environmental Sciences, University of Basel, Basel, 4056, Switzerland, [8]School of Biological Sciences, Monash University, Melbourne, Vic. 3800, Australia, [9]Department of Zoology, Centre for Invasion Biology, University of Venda, Thohoyandou, 0950, South Africa, [10]School of Life Sciences College of Agriculture Engineering and Science, University of KwaZulu-Natal, Pietermaritzburg, 3209, South Africa, [11]Laboratorio Ecotono, Centro Regional Universitario Bariloche, Universidad Nacional del Comahue, INIBIOMA-CONICET, Bariloche, Rio Negro 8400, Argentina, [12]School of Animal, Plant and Environmental Sciences, University of the Witwatersrand, Wits, 2050, South Africa

*Correspondence: Tom R. Bishop, Department of Earth, Ocean and Ecological Sciences, University of Liverpool, Liverpool L69 3GP, UK.
E-mail: thomasrhys.bishop@gmail.com

ABSTRACT

Aim In ectotherms, the colour of an individual's cuticle may have important thermoregulatory and protective consequences. In cool environments, ectotherms should be darker, to maximize heat gain, and larger, to minimize heat loss. Dark colours should also predominate under high UV-B conditions because melanin offers protection. We test these predictions in ants (Hymenoptera: Formicidae) across space and through time based on a new, spatially and temporally explicit, global-scale combination of assemblage-level and environmental data.

Location Africa, Australia and South America.

Methods We sampled ant assemblages ($n = 274$) along 14 elevational transects on three continents. Individual assemblages ranged from 250 to 3000 m a.s.l. (minimum to maximum range in summer temperature of 0.5–35 °C). We used mixed-effects models to explain variation in assemblage cuticle lightness. Explanatory variables were average assemblage body size, temperature and UV-B irradiation. Annual temporal changes in lightness were examined for a subset of the data.

Results Assemblages with large average body sizes were darker in colour than those with small body sizes. Assemblages became lighter in colour with increasing temperature, but darkened again at the highest temperatures when there were high levels of UV-B. Through time, temperature and body size explained variation in lightness. Both the spatial and temporal models explained *c.* 50% of the variation in lightness.

Main conclusions Our results are consistent with the thermal melanism hypothesis, and demonstrate the importance of considering body size and UV-B radiation exposure in explaining the colour of insect cuticle. Crucially, this finding is at the assemblage level. Consequently, the relative abundances and identities of ant species that are present in an assemblage can change in accordance with environmental conditions over elevation, latitude and relatively short time spans. These findings suggest that there are important constraints on how ectotherm assemblages may be able to respond to rapidly changing environmental conditions.

Keywords

Assemblage structure, colour, elevation, latitude, lightness, temperature, thermal melanism, thermoregulation.

DOI: 10.1111/geb.12516
http://wileyonlinelibrary.com/journal/geb

INTRODUCTION

Living organisms displays a huge diversity of colour, which has captured the imagination of biologists for centuries. Animals use different patterns and hues of colour to disguise or advertise themselves (Ruxton *et al.*, 2004), attract mates (Andersson, 1994) or thermoregulate (Clusella-Trullas *et al.*, 2007). For ectotherms, which make up the majority of animal species, thermoregulation is of great importance. Ectotherm metabolism is largely dependent on ambient temperature and, because of this, their performance and geographical distribution is strongly influenced by temperature gradients (Buckley *et al.*, 2012). Consequently, the ability to thermoregulate in response to these gradients is critical for ectotherm survival (Heinrich, 1996).

Ectotherm cuticle colour affects thermoregulation through its reflectivity. A dark-coloured or unreflective individual, with high levels of melanin, will heat up faster and achieve higher temperature excesses than a light-coloured individual of the same size and shape (Willmer & Unwin, 1981). The thermal melanism hypothesis is based on this basic biophysical principle, predicting that darker individuals should predominate in low-temperature environments because they will have a higher fitness (Clusella-Trullas *et al.*, 2007). Higher fitness is a consequence of the longer periods of activity available to darker individuals as they are able to warm up and achieve operating temperatures more rapidly (Bogert, 1949; Clusella-Trullas *et al.*, 2007). Indeed clines in melanism along temperature gradients have been reported in several taxa (e.g. butterflies, dragonflies, reptiles, springtails), across a range of spatial scales and at both intra- and interspecific levels (Rapoport, 1969; Zeuss *et al.*, 2014). Whilst these effects are a direct result of melanin pigmentation, the melanogenesis pathway itself may also influence cold resistance pleiotropically through its effects on energy homeostasis and metabolic rates (Ducrest *et al.*, 2008).

A key assumption of the thermal melanism hypothesis is that individuals have the same size and shape, yet in reality body size and shape vary greatly within and between species. This is important, as body size is a critical factor in determining ectotherm heat budgets. Larger bodies gain and lose heat more slowly than smaller bodies, but also reach higher temperature excesses (Stevenson, 1985). This size effect underpins wide-ranging biogeographical predictions such as Bergmann's rule, which states that organisms should be larger in cold environments (Chown & Gaston, 2010).

The effects of colour and body size on ectotherm thermoregulation are expected to interact. Being large in a cold environment may be advantageous in terms of heat conservation, but it also means that the animal in question will heat up relatively slowly. This inverse body mass–heating relationship has been used as an explanation for the apparent lack of support for Bergmann's rule in ectotherms (Pincheira-Donoso, 2010). Melanism increases the rate at which heat is gained, so may provide a mechanism by which ectotherms could overcome the limitations of a large body size to operate more effectively in a cold environment (Clusella-Trullas *et al.*, 2007). This melanism–body size interaction is predicted from both theory and experiments (Stevenson, 1985; Shine & Kearney, 2001) and has been shown to operate across large geographical scales in ectotherms (Schweiger & Beierkuhnlein, 2015). We therefore expect both body size and ambient temperature to explain variation in ectotherm coloration – darker forms should be larger and occur more frequently in cold environments.

In addition to these thermoregulatory effects, colour, and specifically melanin, has long been linked with a protective role against harmful ultraviolet-B (UV-B) radiation. UV-B can cause a range of deleterious direct effects in ectotherms. These include genetic and embryonic damage, and indirect effects through changes in host plant morphology and biochemistry (Hodkinson, 2005; Beckmann *et al.*, 2014; Williamson *et al.*, 2014). Both experiments (Wang *et al.*, 2008) and correlative studies (Bastide *et al.*, 2014) have provided evidence that melanistic individuals or species can be favoured under conditions of high UV-B. Gloger's rule (Gaston *et al.*, 2008), that endotherms should be darker at low latitudes, suggests that pigmentation provides protection against a range of factors including UV-B irradiance. Patterns in accordance with Gloger's rule and the influence of UV-B have been observed in a number of endotherms (Caro, 2005) and, more recently, in plants (Koski & Ashman, 2015).

The biophysical principles underlying how temperature, body size and UV-B radiation may affect ectotherm colour are understood and accepted at the level of the individual or the species (e.g. Kingsolver, 1995; Ellers & Boggs, 2004). It is unknown, however, to what extent these effects scale to the assemblage level and how important they are at broad spatial and temporal scales. Understanding assemblage-level variation in colour is important as it can reveal how traits influence the performance of species in different environments. In addition, assemblage analyses can generalize across the individualistic responses of each species (Millien *et al.*, 2006). Assemblage-level variation represents changes in the relative abundances of different species – this reflects which trait values appear to be successful under a given set of environmental conditions. In the search for general rules in ecology, rising above the contingencies of extreme behaviours, physiologies or morphologies of individual species is crucial (Chown & Gaston, 2015).

Here, we test if temperature, body size and UV-B can explain variation in cuticle colour of ant (Hymenoptera: Formicidae) assemblages – specifically, how light or dark the colour is. Ants are a diverse, numerically dominant and ecologically important group of insects (Hölldobler & Wilson, 1990) with a wide range of body colours (e.g. http://www.antweb.org). We sampled ant assemblages across replicated elevational gradients on three continents and over multiple years. This design is novel and powerful, for two reasons. First, the combined use of assemblage data,

elevational gradients and continental variation provides broad-ranging yet fine-scale insight across a huge range of environmental conditions and geographies. This combination of fine grain and large extent is rarely achieved (Beck *et al.*, 2012). Second, our use of time-series data provides greater power to assign mechanistic links between cuticle lightness, temperature, body size and UV-B than spatial data alone would.

If cuticle lightness has a thermoregulatory and protective role then we would expect that average cuticle lightness will be: (1) positively related to temperature, (2) negatively related to average body size, and (3) negatively related to UV-B radiation. We test all three predictions across space at a global scale, but only the first two through time.

METHODS

Ant assemblage data

Ant assemblage data were compiled from 14 elevational transects within eight mountain ranges and across three continents (Table 1). Ant assemblages were sampled using pitfall traps in almost exactly the same way across all locations. In South Africa and Lesotho, pitfall traps were arranged into a 10 m × 40 m grid. Four grids were placed in each elevational band with grids being separated by at least 300 m. Traps were 55 mm in diameter and used a 50% ethylene glycol or propylene glycol solution to preserve trapped specimens (Botes *et al.*, 2006; Munyai & Foord, 2012; Bishop *et al.*, 2014). Sampling grids in Australia were of the same dimensions, but those within the same elevation were separated by at least 100 m. In Argentina, a sampling grid consisted of nine pitfall traps arranged in a 10 m × 10 m grid, with each trap separated from the next by 5 m. A single grid was used at each elevation. Traps had a diameter of 90 mm and used a 40% propylene glycol solution to preserve specimens (Werenkraut *et al.*, 2015). Specimens were transferred into 70–80% ethanol in the laboratory and identified to morphospecies or species level, where possible. Hereafter, all morphospecies and species are collectively referred to as species.

All transects were sampled during the austral summer (November–May). Each transect was sampled during a single season, except those in the Maloti-Drakensberg, Cederberg and Soutpansberg regions of South Africa. These transects were been sampled biannually in two seasons for a number of years. These long-term data are only used in the analysis of temporal patterns (see below). For the analysis of spatial patterns, only a single summer sampling period was used. For the Maloti-Drakensberg, Cederberg and Soutpansberg a single year was randomly chosen for the analysis of spatial patterns. The Argentinian transects were also sampled over 2 years but only data from 2006 are used here (Werenkraut *et al.*, 2015). Both years showed the same pattern.

In this study, a sampling grid is considered to be an independent assemblage of ants. We did not pool replicate assemblages within elevational bands. Apart from testing for phylogenetic signal at the genus level, all analyses are performed at the assemblage level. Two hundred and seventy-four assemblages were available for the main spatial analysis after some assemblages had been removed because they did not contain any ants, or environmental data could not be gathered for them.

Lightness data

The colour of each ant species was classified categorically by eye using a predetermined set of colours (see Appendix S1 in the Supporting Information). This method allows for a simple and standardized assessment of colour without the need

Table 1 Details on the geographical and elevational characteristics of the transects used in this study

Continent	Mountain range	Transect	Lowest point (m a.s.l.)	Highest point (m a.s.l.)	No. of elevations	Assemblages per elevation	Species richness	References
Africa	Maloti-Drakensberg	Sani Pass	900	3000	8	4	92	Bishop *et al.* (2014, 2015)
	Soutpansberg	North Aspect	800	1700	5	4	129	Munyai & Foord (2012, 2015)
		South Aspect	900	1600	5	4–8		
	Cederberg	East Aspect	500	1800	6	4	94	Botes *et al.* (2006)
		West Aspect	250	1900	10	4		
	Mariepskop	Mariepskop	700	1900	5	4	92	Tshivhandekano & Robertson (unpublished)
Australia	Snowy Mountains	Back Perisher	400	2000	9	4	109	Gibb *et al.* (unpublished)
	Ben Lomond Plateau, Tasmania	Stack's Bluff	400	1400	6	1–3	12	Gibb *et al.* (unpublished)
	MacDonnell Ranges	Mt Zeil	600	1400	5	4	49	Gibb *et al.* (unpublished)
South America	Andes, north-west Patagonia	Bayo	900	1700	9	1	15	Werenkraut *et al.* (2015)
		Chall-Huaco	900	2000	12	1		
		La Mona	800	1800	11	1		
		Lopez	800	1800	10	1		
		Pelado	800	1800	8	1		

for specialist imaging equipment. The colour of the head, mesosoma and gaster for six individuals of every species in the dataset was recorded. We focused only on the colour of the cuticle and ignored any colouration offered by hairs. The most common colour across all body parts and individuals was assigned as the dominant colour for each species. Each categorical colour was associated with a set of RGB (red, blue and green) values which were extracted from the original colour wheels using the image editing software paint.NET (v.4.0.3). RGB values were converted into HSV (hue, saturation and value) format using the 'rgb2hsv' function in R. The HSV model is a common cylindrical-coordinate representation of colour where hue describes the dominant wavelength, saturation indicates the amount of hue present in the colour and the value sets the amount of light in the colour. Only lightness (v, or value, in HSV) is analysed here. A standardized set of 71 photographs from AntWeb (http://antweb.org/) was used to assess observer error. Error was low (Appendix S1), with the standard error of lightness values estimated from different observers on the same photograph averaging *c.* 0.04. The five observers in this study tended to assign the same lightness value to the same image.

Body size data

The body size of each species was measured as Weber's length. This is the distance between the anterodorsal margin of the pronotum and the posteroventral margin of the propodeum (Brown, 1953). Weber's length was measured to the nearest 0.01 mm using ocular micrometers attached to stereomicroscopes. The highest level of magnification that allowed the entire mesosoma of the specimen to be fitted under the range of the ocular micrometer was used. Only minor workers were measured. Six specimens for each species were measured where possible. Physical specimens were not available for eight species from the Cederberg transects. For these species Weber's length was measured using high-resolution images from AntWeb (http://www.antweb.org) and from existing taxonomic publications (Mbanyana & Robertson, 2008) using the tpsDig2 morphometric software (http://life.bio.sunysb.edu/morph).

Weber's length was not available for the ant species from the MacDonnell Ranges. Instead, it was estimated for these species using the relationship between head width, head length and Weber's length. All three of these traits were available for the Australian Snowy Mountains and Tasmanian ants. Only head width and head length were available for the MacDonnell Ranges ants. Multivariate imputation by chained equations (MICE; Buuren & Groothuis-Oudshoorn, 2011) was performed to estimate the missing Weber's length for these species (Appendix S2).

Temperature data

Global environmental data

Estimates of air temperature for all of the assemblages from January to March (the peak of the austral summer) were extracted from the WorldClim dataset at 30 arcsec resolution (Hijmans *et al.*, 2005). Levels of UV-B irradiance for all assemblages were extracted from the glUV dataset (Beckmann *et al.*, 2014). Mean UV-B irradiances were calculated using data from January to March.

Data loggers

At all transects in Argentina and at two ranges in southern Africa (Maloti-Drakensberg and Soutpansberg) data loggers were used to record daily temperature. In Argentina, a single HOBO H8 logger (Onset Computer Corporation, MA, USA) was placed at ground level in the centre of each replicate block during the sampling months (Werenkraut *et al.*, 2015). In the two southern African sites Thermocron iButtons (Semiconductor Corporation, Dallas/Maxim, TX, USA) were buried 10 mm below ground level at two replicate blocks (of a possible four) in each elevational band (Munyai & Foord, 2012; Bishop *et al.*, 2014). All temperature data were inspected for cases where the data loggers had been exposed to direct sunlight or had clearly malfunctioned. The mean temperature for each replicate in the sampling month was calculated. These data logger temperatures were used to validate the temperature estimates from microclim (Kearney *et al.*, 2014). Furthermore, the data from southern Africa were used to investigate temporal trends (see below).

Statistical methods

All data manipulation and analyses took place in the R statistical environment (R Core Team, 2014).

Phylogenetic signal

A genus-level, time-calibrated ant phylogeny derived from Moreau & Bell (2013) was used to estimate the phylogenetic signal of lightness and body size using Pagel's λ (Pagel, 1999) and Blomberg's K (Blomberg *et al.*, 2003). Lightness and body size traits were averaged at the genus level to test for signal. A likelihood ratio test was used to assess if there was a significant departure of these statistics from zero (no phylogenetic signal). This was done using the 'phytools' package in R (Revell, 2012). In this study 77.4% of the genera were present on the phylogeny. Genera missing from the phylogeny were omitted from this analysis.

Assemblage-level lightness and body size

Assemblage weighted means (AWM) of lightness and body size were calculated for each assemblage (n = 274) according to:

$$\mathrm{AWM} = \sum_{i=1}^{S} p_i x_i$$

where S is the number of species in an assemblage, p_i is the proportional abundance of each species and x_i is the trait value (lightness or body size) of each species.

Data loggers versus WorldClim

The relationship between the mean temperatures collected through the data loggers and those extracted from WorldClim was investigated using Type II major axis regression. This was done with the 'lmodel2' package in R (Legendre, 2008). If the 95% confidence intervals of the intercept and slope encompassed zero and one, respectively, this would indicate that the WorldClim temperature data accurately matched that from the data loggers. The significance of the correlation coefficient was assessed using 999 permutations.

There was a strong correlation between the temperature values obtained from the data loggers and those extracted from WorldClim ($r = 0.94$, $P < 0.001$; Appendix S4). The intercept did not differ from zero (95% CI intercept = −2.69, 0.03) while the slope differed from one, if only slightly (95% CI slope = 1.11, 1.13). Thus WorldClim temperatures slightly underestimated the data logger temperatures.

Spatial patterns

Linear mixed models (LMMs) were used to assess how much variation in assemblage-weighted lightness could be explained by WorldClim estimates of temperature, the amount of UV-B radiation and assemblage-weighted mean body size. Modelling was done using the 'lme4' package in R (Bates *et al.*, 2014). A term for the temperature–UV-B interaction was also fitted. As temperature correlates positively with UV-B in our dataset ($r = 0.81$, $P < 0.001$), UV-B was regressed on temperature and the residuals of this relationship were used as the UV-B variable. All explanatory variables were scaled and standardized to allow greater interpretability of the regression coefficients (Schielzeth, 2010). Explanatory variables were coded as second-order orthogonal polynomials to detect curvature in the relationships between them and assemblage-weighted lightness. A nested random effects structure of transect within mountain range within continent was used to account for the geographical configuration of the study sites. The response variable of assemblage-weighted lightness was logit transformed to meet Gaussian assumptions. An information theoretic approach was used to assess models with different combinations of the explanatory variables. Bias corrected Akaike information criterion (AIC_c) values were used to compare models. Marginal (due to fixed effects only) and conditional (due to fixed effects and random effects) R^2 values were calculated for each model (Bartoń, 2013; Nakagawa & Schielzeth, 2013). Type III tests using Wald X^2 statistics were used to assess the significance of the predictors in the best model. Each of the 274 observations in this analysis was an independent assemblage of ants.

Common and rare species

Two further spatial analyses took place to disentangle which species were driving the spatial patterns. For each assemblage, common species were defined as those making up 90% of the individuals. The remainder were classed as rare species. We chose this rule to reflect the extremes of the common–rare spectrum. Assemblage-weighted lightness and body size were then recalculated using either only the common species or only the rare species in each assemblage. Modelling of the modified assemblage-weighted lightness (and modified assemblage-weighted body size) took place separately for the common and the rare species, as described above for the complete spatial analysis.

Temporal patterns

The Maloti-Drakensberg and Soutpansberg ant assemblages and temperature data are available for multiple years (7 and 5, respectively). A LMM was used to relate average lightness to average temperature and body size for each assemblage across all years. Modelling took place as described for the spatial analysis but the random effects structure was modified to take into account temporal pseudoreplication: sampling grid was nested within transect within mountain range. This model allows us to detect whether the lightness values of each assemblage covary according to temporal changes in temperature and body size. There were 206 observations in this analysis representing 41 different replicate assemblages sampled over a number of years (Maloti-Drakensberg = 19 assemblages over 7 years, Soutpansberg = 22 assemblages over 5 years). There were 243 space/time samples available but 37 caught no ants, leading to 206 useable observations.

RESULTS

Across all transects 592 ant species were collected (Table 1). These species spanned the full range of possible lightness values (0–1). Weber's length varied from 0.25 to 6.48 mm. Assemblage-weighted lightness ranged from 0 to 0.9 whilst assemblage-weighted body size ranged from 0.62 to 2.88 mm.

Phylogenetic signal

Lightness was not significantly conserved across the phylogeny – closely related genera do not resemble each other more so than would be expected by chance (Pagel's $\lambda = 0.32$, $P = 0.06$; Blomberg's $K = 0.59$, $P = 0.13$). Body size was conserved, however (Pagel's $\lambda = 0.81$, $P = 0.001$; Blomberg's $K = 0.86$, $P = 0.002$). This signal was due to genera in the Ponerinae subfamily tending to be larger than those in other subfamilies (Appendix S3). We do not consider this to confound the analyses because proportional representation of Ponerinae in the sampled assemblages does not correlate strongly with their average body sizes ($r = -0.003$, $P = 0.96$). A strong correlation between the proportions of an assemblage that are ponerines and average body size would have indicated that this phylogenetic signal was influencing the results.

Spatial patterns

The best spatial model was also the most complicated. It contained the main effects of temperature, residual UV-B, body size and also included an interaction between

Table 2 Comparative and summary statistics for linear mixed models explaining variation in ant assemblage colour across space or through time.

Model	d.f.	LL	AIC_c	ΔAIC_c	$wAIC_c$	R^2_m	R^2_c
Spatial							
$\sim (BS + BS^2) + (T + T^2) \times (UV + UV^2)$	15	−301.59	635.03	0.00	1.00	0.48	0.62
$\sim (BS + BS^2) + (T + T^2) + (UV + UV^2)$	11	−315.07	653.14	18.11	0.00	0.38	0.56
$\sim (T + T^2) \times (UV + UV^2)$	13	−313.37	654.14	19.11	0.00	0.41	0.59
$\sim (BS + BS^2) + (T + T^2)$	9	−321.63	661.94	26.90	0.00	0.43	0.61
$\sim (BS + BS^2) + (UV + UV^2)$	9	−322.69	664.05	29.02	0.00	0.21	0.62
$\sim (T + T^2) + (UV + UV^2)$	9	−325.24	669.17	34.14	0.00	0.28	0.52
$\sim (T + T^2)$	7	−328.97	672.36	37.33	0.00	0.36	0.59
$\sim (UV + UV^2)$	7	−335.04	684.50	49.47	0.00	0.14	0.62
$\sim (BS + BS^2)$	7	−347.08	708.58	73.55	0.00	0.07	0.41
~ 1	5	−356.71	723.64	88.61	0.00	0.00	0.44
Temporal							
$\sim (BS + BS^2) + (T + T^2)$	10	−112.24	245.60	0.00	0.96	0.49	0.74
$\sim (BS + BS^2)$	8	−117.65	252.03	6.43	0.04	0.36	0.69
$\sim (T + T^2)$	8	−145.36	307.46	61.85	0.00	0.11	0.59
~ 1	6	−149.12	310.66	65.06	0.00	0.00	0.61

Predictors were all second-order orthogonal polynomials and included average body size ($BS + BS^2$), average summer temperature ($T + T^2$) and average residual UV-B radiation ($UV + UV^2$). The temperature variables were derived from WorldClim for the spatial models and from data loggers in the temporal models. Listed are the degrees of freedom (d.f.), maximum log-likelihood (LL), Akaike's bias corrected information criterion (AIC_c) and its change relative to the top ranked model (ΔAIC_c), the model probabilities ($wAIC_c$) and the marginal and conditional R^2s. Marginal R^2 (R^2_m) is the amount of variation explained by the fixed effects, conditional R^2 (R^2_c) is that explained by the fixed and random effects.

temperature and UV-B (Table 2). All variables apart from the main effect of residual UV-B radiation were significant according to Type III Wald X^2 tests (Table 3). Assemblage-weighted lightness declined with increasing assemblage-weighted body size (Fig. 1a). At low levels of residual UV-B, assemblage-weighted lightness increased with increasing temperature. At high levels of residual UV-B the relationship between lightness and temperature was unimodal – at higher temperatures lightness declined (Fig. 1b). Species richness did not influence these results given the small amount of variation in assemblage lightness that species richness is able to explain ($R^2_m = 0.02$, $R^2_c = 0.38$; Appendix S5). The same results were found when using microclim (Kearney *et al.*, 2014) temperature data rather than WorldClim data (Appendix S6).

Table 3 Test statistics (χ^2), degrees of freedom (d.f.) and *P*-values from Type III Wald tests on the best spatial and temporal models (top ranked spatial and temporal models from Table 2).

Spatial	χ^2	d.f.	*P*
$T + T^2$	29.77	2	<0.001
$UV + UV^2$	3.01	2	0.22
$BS + BS^2$	24.81	2	<0.001
$(T + T^2) \times (UV + UV^2)$	29.43	4	<0.001
Temporal			
$T + T^2$	16.48	2	<0.001
$BS + BS^2$	87.85	2	<0.001

Explanatory variables were second-order orthogonal polynomials and included average body size ($BS + BS^2$), average summer temperature ($T + T^2$) and average residual UV-B radiation ($UV + UV^2$). The temperature variables were derived from WorldClim for the spatial models and from data loggers in the temporal models.

Common and rare species

The best model for common species was exactly the same as the overall spatial model (which used all species) and also explained a similar amount of variance ($R^2_m = 0.47$, $R^2_c = 0.69$; Appendix S7). For the rare species, the best model contained assemblage body size and residual UV-B. Lightness declined with increasing average body size and formed a U-shaped relationship with residual UV-B. This model did not explain much variation ($R^2_m = 0.15$, $R^2_c = 0.47$; Appendix S7).

Temporal patterns

The best temporal model included both mean temperature and body size (Table 2). Lightness showed a negative relationship with body size (Fig. 2a) and a positive relationship with data logger-derived temperature (Fig. 2b). Both body size and temperature were significant according to Type III Wald X^2 tests (Table 3).

DISCUSSION

Our study shows that broad geographical patterns of cuticle colour in ants are consistent with a role in thermoregulation and a UV-B protection, as predicted by experiment and theory (Stevenson, 1985; Shine & Kearney, 2001; Wang *et al.*,

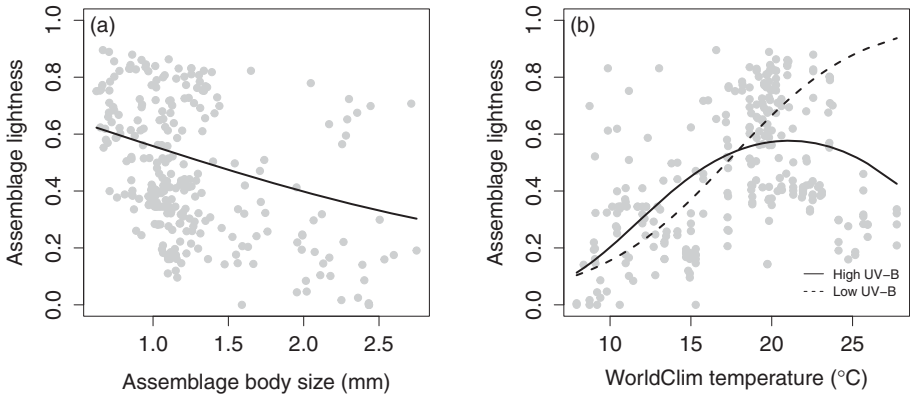

Figure 1 Plots showing the relationship between mean assemblage lightness and body size (a) and mean WorldClim-derived summer temperature (b). Lines display model predictions. In (b) the solid line represents predictions for low levels of UV-B (10th percentile) and the dashed line represents predictions for high UV-B (90th percentile) ($n = 274$). R^2_m (fixed effects) = 0.48, R^2_c (fixed and random effects) = 0.62.

2008). Furthermore, the effects that we detected were at the assemblage level and therefore reflect changes in the relative abundances of species. Generally, the most abundant species are those with a cuticle colour that is best suited, in a thermoregulatory or protective sense (Stevenson, 1985; Shine & Kearney, 2001; Wang *et al.*, 2008), to the prevailing environmental conditions. This suggests that assemblage structure will change as the optimum cuticle lightness changes depending on the climate. Our temporal data show that this can happen over a relatively short time-scale through shifts in species abundance. Such shifts in assemblage structure under predicted levels of climate change may have cascading effects on ecosystem functioning and integrity.

Across space, we find that, on average, assemblages have lighter cuticles in warm environments and darker cuticles where it is cooler. High UV-B irradiance makes a difference where it is hot, and is associated with darker cuticles (Fig. 1b). In addition, assemblage cuticle lightness was negatively correlated with assemblage body size (Fig. 1a). We find similar results through time. Our data show that temporal changes in the assemblage cuticle lightness were negatively related to body size (Fig. 2a) and positively related to temperature (Fig. 2b).

Our data can be interpreted in light of both of the two major contrasting ecogeographical rules that describe and explain colour variation. These are the thermal melanism hypothesis, or Bogert's rule (Clusella-Trullas *et al.*, 2007), and Gloger's rule (Caro, 2005; Millien *et al.*, 2006). The two rules differ in their target animal groups and in their principal underlying mechanisms. The thermal melanism hypothesis is usually applied to ectotherms and proposes that darker colours should dominate in cold environments (usually high latitudes or elevations) because of the thermoregulatory benefits of being dark. Gloger's rule is typically applied to endotherms and states that darker colours are found closer to the equator in warmer environments. This pattern may be caused by UV-B protection, camouflage or thermoregulatory needs – white fur can scatter radiation toward the skin for heat gain whilst dark fur can enhance cooling via evaporation (Caro, 2005; Millien *et al.*, 2006; Koski & Ashman, 2015). Whilst the majority of our dataset supports the thermal melanism hypothesis (ants are darker in colder environments) the significant interaction of temperature and UV-B in our modelling procedure (Fig. 1b, Table 3) suggests that the UV-B protection mechanism of Gloger's rule may also be applicable

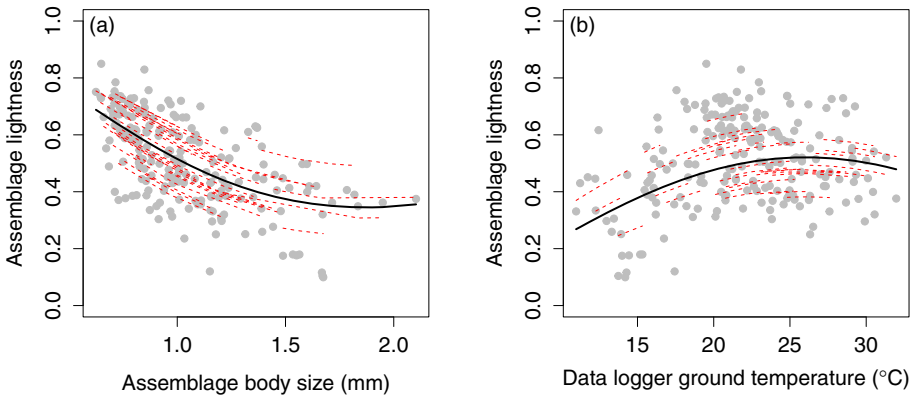

Figure 2 Plots showing the relationship between mean assemblage lightness and body size (a) and mean data logger-derived summer temperature (b) through time for the Maloti-Drakensberg and Soutpansberg mountain ranges of southern Africa ($n = 206$). Solid black lines display the average model predictions. Dashed lines display predictions for each individual assemblage (41 unique assemblages). R^2_m (fixed effects) = 0.49, R^2_c (fixed and random effects) = 0.74.

to ant assemblages (e.g. Bastide *et al.*, 2014; Koski & Ashman, 2015).

Comparable results to ours have been found using multiple species across large areas. For example, European insects show positive relationships between cuticle lightness and temperature (Zeuss *et al.*, 2014), whilst the cuticle lightness of carabid beetles is negatively related to body size across Europe (Schweiger & Beierkuhnlein, 2015). Our results are in agreement with these previous findings, but take them a step further by using assemblage-level data. This provides information on the identities and relative abundances of the species (and their cuticle lightness) that were active at the time of our sampling. As a consequence, the performance of different lightness values in different environments is captured by our assemblage average. This point is illustrated well in our temporal analysis. The same point in space shows different lightness values under different temperatures – species with the correct cuticle lightness are able to rapidly take advantage of altered thermal conditions. The agreement that we find between the spatial and temporal patterns greatly strengthens the power that we have to infer a process of assemblage change mediated by ant physiology than either pattern would in isolation (White *et al.*, 2010).

By restricting our assemblage data to the most common species, we find the same patterns in cuticle lightness. This implies that it is the dominant ant species that are driving the relationships between cuticle lightness, temperature and UV-B. This is important as the dominant species are consuming most of the energy in the system and can structure the rest of the assemblage (Parr, 2008). This finding emphasizes the importance of the abiotic environment in structuring local assemblages and contrasts with the majority of the existing literature on ants (e.g. Cerdá *et al.*, 2013), which has tended to focus on the importance of biotic factors such as competition (but see Gibb, 2011). The importance of the common species in driving these macrophysiological patterns echoes similar findings in macroecology where it is also the common species which drive assemblage diversity patterns (Reddin *et al.*, 2015).

Previous studies on this topic (Zeuss *et al.*, 2014; Schweiger & Beierkuhnlein, 2015), and in macroecology in general (Beck *et al.*, 2012), rarely have the right kinds of data to draw conclusions at the assemblage level. We argue that understanding the fine spatial and temporal scale of variation is crucial for appreciating how, and why, organisms respond to the environment. Most ectotherms do not interact with each other, or their environment, at the 50-km^2 scale. Instead, it is the success of individuals at finer grains that determines population viability and, ultimately, drives ecosystem functioning. It should be noted, however, that despite the large influence that spatial extent and grain size may have in determining geographical patterns (Rahbek, 2005), the relationships between lightness, temperature and body size in our dataset (grain size of *c.* 400 m^2) are consistent with those studies using a much larger grain size (Zeuss *et al.*, 2014; Schweiger & Beierkuhnlein, 2015). This combination of evidence suggests that the thermoregulatory role of colour in ectotherms may scale consistently to: (1) influence the success of individuals (e.g. Ellers & Boggs, 2004), (2) shape assemblage structure (this study) and (3) determine which species are present in the wider regional pool (e.g. Zeuss *et al.*, 2014).

Although our spatial and temporal models explain a large amount of the assemblage-level variation in cuticle lightness in our dataset (*c.* 50% for fixed effects; Table 2), a considerable portion of the variation remains unexplained. There are likely to be two main sources for this variation. The first is methodological. Our use of global surfaces (WorldClim and glUV) in the spatial analysis is likely to have underestimated the true range of temperatures and UV-B levels encountered by the sampled ant assemblages. This could lead to assemblages appearing lighter or darker than expected for their estimated temperatures. This is less of an issue for our temporal analysis as we used data loggers to track temperature. Secondly, we may be under-appreciating the ability of ants to thermoregulate without the use of cuticle colour. A range of other morphological and behavioural mechanisms can play a role in ant thermoregulation. This has been reported mainly for extremely hot conditions. For example, *Cataglyphis* species have been recorded to use specialized reflecting hairs (Shi *et al.*, 2015) to thermoregulate in hot conditions. In addition, ants have been widely reported to forage at cooler times of the day to avoid peak temperatures (Fitzpatrick *et al.*, 2014), which may completely decouple the biophysical link between their morphological thermoregulatory traits and the environment. In cold environments, nest architecture and building materials can keep colonies warm (Hölldobler & Wilson, 1990), but there is little reporting of individual worker traits that allow activity to be maintained in the cold. We assume that these mechanisms are the exception rather than the rule, but this may not be the case.

In summary, we have shown that the structure of assemblages can be driven by the differential performance of species based on their thermoregulatory traits. This finding suggests that ant assemblages will have to shift in ways consistent with thermoregulatory and protective needs as the climate changes. Under warmer conditions, ants should become smaller and lighter coloured. The existing literature largely agrees with this decrease in body size (Sheridan & Bickford, 2011), but currently suggests that darker melanic individuals will tend to be favoured under climate change scenarios (Roulin, 2014). These predicted changes will probably filter certain kinds of species and alter the functional composition and outputs of assemblages.

ACKNOWLEDGEMENTS

We thank the DST-NRF Centre of Excellence for Invasion Biology, the University of Pretoria, Chantal Ferreira, the Mazda Wildlife Fund, Ezemvelo KZN Wildlife and the Lesotho Ministry of Tourism, Environment and Culture for their various roles in supporting the Maloti-Drakensberg, Soutpansberg and

Cederberg transects. The Mariepskop transect was financially supported by the NRF and 19 Helicopter Squadron at Hoedspruit provided logistical support. T.R.B. was supported by a NERC studentship. Theo Evans and Chris Jeffs provided stimulating discussion that much improved the direction of the manuscript. Alexandre Roulin and an anonymous referee provided reviews which improved the final version.

REFERENCES

Andersson, M.B. (1994) *Sexual selection*. Princeton University Press, Princeton, NJ.

Bartoń, K. (2013) *MuMIn: multi-model inference*. R package version 1.15.6. http://cran.r-project.org/package=MuMIn.

Bastide, H., Yassin, A., Johanning, E.J. & Pool, J.E. (2014) Pigmentation in *Drosophila melanogaster* reaches its maximum in Ethiopia and correlates most strongly with ultraviolet radiation in sub-Saharan Africa. *BMC Evolutionary Biology*, **14**, 179.

Bates, D., Maechler, M., Bolker, B., Walker, S., Christensen, R.H.B., Singmann, H. & Dai, B. (2014) *lme4: linear mixed-effects models using Eigen and S4*. R package version 1.1-6. http://cran.r-project.org/package=lme4.

Beck, J., Ballesteros-Mejia, L., Buchmann, C.M., Dengler, J., Fritz, S.A., Gruber, B., Hof, C., Jansen, F., Knapp, S & Kreft, H. (2012) What's on the horizon for macroecology? *Ecography*, **35**, 673–683.

Beckmann, M., Václavík, T., Manceur, A.M., Šprtová, L., Wehrden, H., Welk, E. & Cord, A.F. (2014) glUV: a global UV-B radiation data set for macroecological studies. *Methods in Ecology and Evolution*, **5**, 372–383.

Bishop, T.R., Robertson, M.P., van Rensburg, B.J. & Parr, C.L. (2014) Elevation–diversity patterns through space and time: ant communities of the Maloti-Drakensberg Mountains of southern Africa. *Journal of Biogeography*, **41**, 2256–2268.

Bishop, T.R., Robertson, M.P., van Rensburg, B.J. & Parr, C.L. (2015) Contrasting species and functional beta diversity in montane ant assemblages. *Journal of Biogeography*, **42**, 1776–1786.

Blomberg, S.P., Garland, T., Jr, Ives, A.R. & Crespi, B. (2003) Testing for phylogenetic signal in comparative data: behavioral traits are more labile. *Evolution*, **57**, 717–745.

Bogert, C.M. (1949) Thermoregulation in reptiles, a factor in evolution. *Evolution*, **3**, 195–211.

Botes, A., McGeoch, M.A., Robertson, H.G., van Niekerk, A., Davids, H.P. & Chown, S.L. (2006) Ants, altitude and change in the Northern Cape Floristic Region. *Journal of Biogeography*, **33**, 71–90.

Brown, W.L. (1953) Revisionary studies in the ant tribe Dacetini. *American Midland Naturalist*, **50**, 1–137.

Buckley, L.B., Hurlbert, A.H. & Jetz, W. (2012) Broad-scale ecological implications of ectothermy and endothermy in changing environments. *Global Ecology and Biogeography*, **21**, 873–885.

Buuren, S. & Groothuis-Oudshoorn, K. (2011) mice: multivariate imputation by chained equations in R. *Journal of Statistical Software*, **45**, 1–67.

Caro, T. (2005) The adaptive significance of coloration in mammals. *BioScience*, **55**, 125–136.

Cerdá, X., Arnan, X. & Retana, J. (2013) Is competition a significant hallmark of ant (Hymenoptera: Formicidae) ecology. *Myrmecological News*, **18**, 131–147.

Chown, S.L. & Gaston, K.J. (2010) Body size variation in insects: a macroecological perspective. *Biological Reviews*, **85**, 139–169.

Chown, S.L. & Gaston, K.J. (2015) Macrophysiology – progress and prospects. *Functional Ecology*, **30**, 330–344.

Clusella-Trullas, S., van Wyk, J.H. & Spotila, J.R. (2007) Thermal melanism in ectotherms. *Journal of Thermal Biology*, **32**, 235–245.

Ducrest, A.L., Keller, L. & Roulin, A. (2008) Pleiotropy in the melanocortin system, coloration and behavioural syndromes. *Trends in Ecology and Evolution*, **23**, 502–510.

Ellers, J. & Boggs, C.L. (2004) Functional ecological implications of intraspecific differences in wing melanization in *Colias* butterflies. *Biological Journal of the Linnean Society*, **82**, 79–87.

Fitzpatrick, G., Lanan, M.C. & Bronstein, J.L. (2014) Thermal tolerance affects mutualist attendance in an ant–plant protection mutualism. *Oecologia*, **176**, 129–138.

Gaston, K.J., Chown, S.L. & Evans, K.L. (2008) Ecogeographical rules: elements of a synthesis. *Journal of Biogeography*, **35**, 483–500.

Gibb, H. (2011) Experimental evidence for mediation of competition by habitat succession. *Ecology*, **92**, 1871–1878.

Heinrich, B. (1996) *The thermal warriors: strategies of insect survival*. Harvard University Press, Cambridge, MA.

Hijmans, R.J., Cameron, S.E., Parra, J.L., Jones, P.G. & Jarvis, A. (2005) Very high resolution interpolated climate surfaces for global land areas. *International Journal of Climatology*, **25**, 1965–1978.

Hodkinson, I.D. (2005) Terrestrial insects along elevation gradients: species and community responses to altitude. *Biological Reviews*, **80**, 489–513.

Hölldobler, B. & Wilson, E.O. (1990) *The ants*. Springer-Verlag, Berlin.

Kearney, M.R., Isaac, A.P. & Porter, W.P. (2014) microclim: global estimates of hourly microclimate based on long-term monthly climate averages. *Scientific Data*, **1**, 140006.

Kingsolver, J.G. (1995) Fitness consequences of seasonal polyphenism in western white butterflies. *Evolution*, **49**, 942–954.

Koski, M.H. & Ashman, T.L. (2015) Floral pigmentation patterns provide an example of Gloger's rule in plants. *Nature Plants*, **1**, 5.

Legendre, P. (2008) *lmodel2: model II regression*. R package version 1.7-2. http://cran.r-project.org/package=lmodel2.

Mbanyana, N. & Robertson, H.G. (2008) Review of the ant genus *Nesomyrmex* (Hymenoptera: Formicidae: Myrmicinae) in southern Africa. *African Natural History*, **4**, 35–55.

Millien, V., Kathleen Lyons, S., Olson, L., Smith, F.A., Wilson, A.B. & Yom-Tov, Y. (2006) Ecotypic variation in the context of global climate change: revisiting the rules. *Ecology Letters*, **9**, 853–869.

Moreau, C.S. & Bell, C.D. (2013) Testing the museum versus cradle tropical biological diversity hypothesis: phylogeny, diversification, and ancestral biogeographic range evolution of the ants. *Evolution*, **67**, 2240–2257.

Munyai, T.C. & Foord, S.H. (2012) Ants on a mountain: spatial, environmental and habitat associations along an altitudinal transect in a centre of endemism. *Journal of Insect Conservation*, **16**, 677–695.

Munyai, T.C. & Foord, S.H. (2015) Temporal patterns of ant diversity across a mountain with climatically contrasting aspects in the Tropics of Africa. *PLoS One*, **10**, e0122035.

Nakagawa, S. & Schielzeth, H. (2013) A general and simple method for obtaining R^2 from generalized linear mixed-effects models. *Methods in Ecology and Evolution*, **4**, 133–142.

Pagel, M. (1999) Inferring the historical patterns of biological evolution. *Nature*, **401**, 877–884.

Parr, C.L. (2008) Dominant ants can control assemblage species richness in a South African savanna. *Journal of Animal Ecology*, **77**, 1191–1198.

Pincheira-Donoso, D. (2010) The balance between predictions and evidence and the search for universal macroecological patterns: taking Bergmann's rule back to its endothermic origin. *Theory in Biosciences*, **129**, 247–253.

Rahbek, C. (2005) The role of spatial scale and the perception of large-scale species-richness patterns. *Ecology Letters*, **8**, 224–239.

Rapoport, E. (1969) Gloger's rule and pigmentation of Collembola. *Evolution*, 622–626.

R Core Team (2014) *R: a language and environment for Statistical Computing*. R Foundation for Statistical Computing, Vienna, Austria.

Reddin, C., Bothwell, J. & Lennon, J. (2015) Between-taxon matching of common and rare species richness patterns. *Global Ecology and Biogeography*, **24**, 1476–1486.

Revell, L.J. (2012) phytools: an R package for phylogenetic comparative biology (and other things). *Methods in Ecology and Evolution*, **3**, 217–223.

Roulin, A. (2014) Melanin-based colour polymorphism responding to climate change. *Global Change Biology*, **20**, 3344–3350.

Ruxton, G.D., Sherratt, T.N. & Speed, M.P. (2004) *Avoiding attack*. Oxford University Press, Oxford.

Schielzeth, H. (2010) Simple means to improve the interpretability of regression coefficients. *Methods in Ecology and Evolution*, **1**, 103–113.

Schweiger, A.H. & Beierkuhnlein, C. (2015) Size dependency in colour patterns of Western Palearctic carabids. *Ecography*, doi: 10.1111/ecog.01570.

Sheridan, J.A. & Bickford, D. (2011) Shrinking body size as an ecological response to climate change. *Nature Climate Change*, **1**, 401–406.

Shi, N.N., Tsai, C.C., Camino, F., Bernard, G.D., Yu, N. & Wehner, R. (2015) Keeping cool: enhanced optical reflection and heat dissipation in silver ants. *Science*, **349**, 298–301.

Shine, R. & Kearney, M. (2001) Field studies of reptile thermoregulation: how well do physical models predict operative temperatures? *Functional Ecology*, **15**, 282–288.

Stevenson, R. (1985) The relative importance of behavioral and physiological adjustments controlling body temperature in terrestrial ectotherms. *The American Naturalist*, **126**, 362–386.

Wang, Z., Liu, R., Wang, A., Du, L. & Deng, X. (2008) Phototoxic effect of UVR on wild type, ebony and yellow mutants of *Drosophila melanogaster*: life span, fertility, courtship and biochemical aspects. *Science in China Series C: Life Sciences*, **51**, 885–893.

Werenkraut, V., Fergnani, P.N. & Ruggiero, A. (2015) Ants at the edge: a sharp forest-steppe boundary influences the taxonomic and functional organization of ant species assemblages along elevational gradients in northwestern Patagonia (Argentina). *Biodiversity and Conservation*, **24**, 287–308.

White, E.P., Ernest, S.K.M., Adler, P.B., Hurlbert, A.H. & Lyons, S.K. (2010) Integrating spatial and temporal approaches to understanding species richness. *Philosophical Transactions of the Royal Society B: Biological Sciences*, **365**, 3633–3643.

Williamson, C.E., Zepp, R.G., Lucas, R.M., Madronich, S., Austin, A.T., Ballaré, C.L., Norval, M., Sulzberger, B., Bais, A.F. & McKenzie, R.L. (2014) Solar ultraviolet radiation in a changing climate. *Nature Climate Change*, **4**, 434–441.

Willmer, P. & Unwin, D. (1981) Field analyses of insect heat budgets: reflectance, size and heating rates. *Oecologia*, **50**, 250–255.

Zeuss, D., Brandl, R., Brändle, M., Rahbek, C. & Brunzel, S. (2014) Global warming favours light-coloured insects in Europe. *Nature Communications*, **5**, 3874. [24866819]

SUPPORTING INFORMATION

Additional supporting information may be found in the online version of this article at the publisher's web-site:

Appendix S1 Colour assignment.
Appendix S2 Multivariate imputation using chained equations (MICE) of MacDonnell Ranges body size.
Appendix S3 Phylogenetic signal.
Appendix S4 Relationship between temperature values obtained from data loggers in the Maloti-Drakensberg, Soutpansberg and Patagonian Andes and those extracted from WorldClim.
Appendix S5 Species richness effects.
Appendix S6 Modelling of lightness across space using microclim temperature data.
Appendix S7 Modelling of lightness across space for common and rare species.

Figure S1.1 Colour wheels used to categorize the colour of ant species across the three continents.
Figure S1.2 Histograms showing the standard errors of lightness values estimated for the head, mesosoma and gaster by the five observers used in this study on a set of 71 photographs of ants from http://antweb.org/.
Figure S2.1 Plots showing relationship between morphological traits for Australian ants from the Snowy Mountains, MacDonnell Ranges and Ben Lomond Plateau, Tasmania.
Figure S3.1 Plot showing the distribution of average genus body sizes across the ant subfamilies present in this study.
Figure S4.1 Relationship between temperature values obtained from data loggers and those extracted from WorldClim.
Figure S5.1 Stacked density plot showing the distribution of lightness values for each mountain range.
Figure S5.2 Plot showing the relationship between assemblage lightness and species richness.
Figure S6.1 Relationship between temperature values obtained from data loggers and those extracted from microclim.
Figure S6.2 Plots showing the relationship between assemblage lightness and body size and average microclim-derived summer temperature.
Figure S7.1 Plots showing the relationship between assemblage lightness and body size and average WorldClim-derived summer temperature.
Figure S7.2 Plots showing the relationship between assemblage lightness and body size and residual summer UV-B.
Table S6.1 Comparative and summary statistics for linear mixed models explaining variation in ant assemblage colour across space.
Table S6.2 Test statistics (χ^2), degrees of freedom and *P*-values from Type III Wald tests on the best spatial model (top ranked from Table S6.1).
Table S7.1 Comparative and summary statistics for linear mixed models explaining variation in ant assemblage colour across space for either common or rare species.
Table S7.2 Test statistics (χ^2), degrees of freedom and *P*-values from Type III Wald tests on the best spatial models for common and rare species subsets (top ranked from Table S7.1).

BIOSKETCH

Tom R. Bishop is interested in using morphology and physiology to understand the distribution of biological diversity, particularly that of the ants.

Editor: Daniel Pincheira-Donoso